A MULTISCALE DAMAGE MODEL FOR COMPOSITE MATERIALS USING A FFT-BASED METHOD

JOHANNES SPAHN[*†], HEIKO ANDRÄ[*†], MATTHIAS KABEL[*] AND RALF MÜLLER[†]

[*]Fraunhofer Institute for Industrial Mathematics (ITWM)
Department Flow and Material Simulation
Fraunhofer-Platz 1, 67663 Kaiserslautern, Germany
e-mail: spahn@itwm.fraunhofer.de, web page: http://www.itwm.fraunhofer.de

[†]Institute of Applied Mechanics
Technische Universität Kaiserslautern
Gottlieb-Daimler-Straße, 67653 Kaiserslautern, Germany
web page: http://www.mechanik.mv.uni-kl.de

Key words: Multiscale Analysis, Computational Homogenization, Continuum Damage Mechanics, FFT, Composite Materials, Localization

Abstract. Modeling failure and progressive damage of composite materials presents a challenging task and is currently subject of many research activities in the field of computational mechanics. Conventional methods which assume constant material coefficients or global failure criteria, are in many cases not sufficient to predict the appropriate mechanical material response. Composite failure occurs as a result of complex meso-structural damage mechanisms and therefore it is preferable to capture these nonlinear material effects directly on a finer scale. Hence, recent multiscale modeling and simulation techniques were developed to consider the mesoscopic material behavior. In this contribution we propose an alternative multiscale approach similar to FE^2. Nonlinear material effects caused by progressive damage behavior are captured on a finer length scale. The constituents are modeled explicitly and simple isotropic damage laws are used to describe the constitutive behavior. Hence, the resulting material response is based on genuine physical effects and only a few material parameters are required which can be measured directly in physical experiments. The fine scale problem (material level) is reformulated into an integral equation of Lippmann-Schwinger type and solved efficiently using the fast Fourier transformation (FFT). The calculation is carried out on a regular voxel grid which can be obtained from 3D images like tomographies without using any complicated mesh generation. Furthermore, the fine scale problem is integrated in a standard Finite Element framework which is used to solve the macroscopic BVP (component level).

1 INTRODUCTION

Fiber-reinforced composites possess a complex material response, which is not sufficiently understood at present time. Especially modeling failure and progressive damage of composite materials, presents a major challenge in current research activities. Composite failure occurs as a result of a variety of complex mesostructural damage mechanisms, such as matrix damage, fiber pull out and fiber breakage.

Recently, phenomenological macroscale models are state of the art for failure investigations in many applications. These models assume homogeneous material behavior and are usually based on macroscopic failure criteria. Disadvantages are the extensive identification of material parameters in dependence of the material structure and the loading conditions. Physical phenomena occurring on a finer length scale are not considered.

A more accurate approach is to capture the nonlinear material effects directly on a finer scale. Therefore, the mesostructural constituents are modeled explicitly on the interesting scale. The resulting material response is based on genuine physical effects and consequently arbitrary complex non-proportional, multiaxial loading conditions can be captured. Moreover, simple (isotropic) constitutive laws are used to define the material behavior of the mesostructural constituents and the required parameters can be measured directly in physical experiments. However, the detailed resolution of the mesostructural constituents leads to a fine discretization of the computational model and thus to large algebraic systems with many degrees of freedom. Recent multiscale modeling and simulation techniques were developed to restrict the computational effort to an acceptable extent and nevertheless capture the mesomechanical material effects in a proper way [8].

One well-known method is the FE^2 approach [4]. The scales are solved separately and each macroscopic point is equipped with a certain mesostructure. Therefore the constitutive equation for the coarse scale is replaced by an additional mesoscopic boundary value problem (BVP) which is solved on a representative volume element (RVE).

In this work an alternative method is presented which uses the Fast Fourier Transformation (FFT) to solve an equivalent elastic meso BVP (material level). A periodic BVP known from ordinary elasticity problems is reformulated in an integral equation of the so called Lippmann-Schwinger type [20, 9]. This method was introduced by Moulinec and Suquet [14, 15]. Advantages of this method are its efficiency in terms of memory consumption and computational time. Further the calculation is carried out on a regular voxel grid and could therefore directly be applied to calculate homogenized quantities on 3D images like tomographies without using any complicated mesh generation. The fine scale problem can easily be integrated in a standard Finite Element framework which is used to solve the macroscopic BVP (component level).

In the first part of this paper the constitutive equation and the numerical solution of the mesoscale model are introduced. The second part presents the coupling technique of the two geometrical scales and the principles of numerical homogenization are explained. Finally the paper closes with numerical examples of some simple scale coupling problems.

2 MESOSCALE MODEL

In this section the constitutive equation and the numerical solution of the mesoscopic BVP is introduced.

2.1 Isotropic Nonlocal Damage Model

In this work we use a nonlocal formulation of a strain based continuum damage model according to Simo & Ju [18], whereby any other constitutive model can be used to describe the material behavior of the mesoscopic constituents.

In the context of Continuum Damage Mechanics (CDM), Kachanov [7] introduced an internal variable d ranging from 0 to 1. While $d = 0$ represents the undamaged state, $d = 1$ describes the status of completely failed material. The constitutive equation is derived from a thermodynamic state potential, the Helmholtz free energy ψ:

$$\psi \;=\; \frac{1}{2}(1-d)\,\boldsymbol{\varepsilon} : \mathbb{C}_{el} : \boldsymbol{\varepsilon} \tag{1}$$

$$\boldsymbol{\sigma} \;=\; \frac{\partial \psi}{\partial \boldsymbol{\varepsilon}} = (1-d)\,\mathbb{C}_{el} : \boldsymbol{\varepsilon} \,, \tag{2}$$

where $\mathbb{C}_{el}$ is the isotropic elasticity tensor. The specific strain energy $\frac{1}{2}\,\boldsymbol{\varepsilon} : \mathbb{C}_{el} : \boldsymbol{\varepsilon}$ is the thermodynamic force Y associated with the internal state variable d:

$$Y = -\frac{\partial \psi}{\partial d} = \frac{1}{2}\,\boldsymbol{\varepsilon} : \mathbb{C}_{el} : \boldsymbol{\varepsilon} \,. \tag{3}$$

A damage criterion f controls the state of damage, which is in the case of growing damage described by a monotonic function $\phi(Y)$:

$$f = \phi(Y) - d \;\leq 0 \quad \begin{cases} f & < & 0 \quad \text{elastic} \\ f & = & 0 \quad \text{damage}\,. \end{cases} \tag{4}$$

An analytical integration of the evolution law yields an exponential expression for the growing damage variable d:

$$d = \phi(Y) = 1 - \mathrm{e}^{(-H(\tilde{\varepsilon}_{(Y)} - Y_0))} \qquad d \in [0,1)\,. \tag{5}$$

In the equation above the material parameters H as the damage hardening modulus and Y_0 as the initial damage threshold are introduced. According to Simo & Ju [18] the strain energy Y is replaced by an equivalent strain measurement $\tilde{\varepsilon}_{(Y)}$ which is obtained by a small modification of Y, namely the energy norm of the strain tensor:

$$\tilde{\varepsilon}_{(Y)} = \sqrt{2Y} = \sqrt{\boldsymbol{\varepsilon} : \mathbb{C} : \boldsymbol{\varepsilon}}\,. \tag{6}$$

There exist several proposals to calculate the equivalent strain [10, 12]. Choosing the energy norm of the strain tensor as an equivalent strain measurement in conjunction with

the thermodynamic consistent (associated) damage formulation, ensures the symmetry of the tangential material moduli [18].

Increasing damage leads to local softening behavior, the tangential material stiffness becomes negative and consequently strain localization effects occur. The strain localizes in certain regions, while the surrounding area gets unloaded. The size of the localizing area is related to the spatial resolution of the mesh and consequently the solution becomes dependent on the existing discretization [3]. The reason is the loss of ellipticity of the governing differential equation and consequently the loss of stability and uniqueness of the solution [17].

In order to avoid mesh dependence of the computational model, regularization methods are used. In this context enhanced models enriched by spatial gradients of the field variables were developed (e.g. [2]). In this work a nonlocal approach according to [16] is used. Hereby the damage variable $\bar{d}$ is averaged over its surrounding area and integrated in the constitutive equation:

$$\boldsymbol{\sigma} = (1 - \bar{d}) \, \mathbb{C}_{el} : \boldsymbol{\varepsilon} \ . \tag{7}$$

The averaging is performed by applying a Gaussian weight function W on the damage variable d on certain points $\boldsymbol{y}$ in the surrounding area:

$$\bar{d}(\boldsymbol{x}) \;\; = \;\; \frac{1}{\displaystyle\int_V W(\boldsymbol{x}, \boldsymbol{y}) dV(\boldsymbol{y})} \int_V W(\boldsymbol{x}, \boldsymbol{y}) \, d(\boldsymbol{y}) \; \mathrm{d}V(\boldsymbol{y}) \tag{8}$$

$$W(\boldsymbol{x}, \boldsymbol{y}) \;\; = \;\; \frac{1}{(2\pi)^{2/3} l^3} \exp\left(-\frac{||\boldsymbol{x} - \boldsymbol{y}||^2}{2l^2} \right) \ . \tag{9}$$

It is mentioned here, that by this procedure a length scale l is introduced in the damage model. To assure mesh independent solutions the discretization must be able to resolve this length l.

2.2 Equivalent BVP and FFT-based Numerical Solution

For computing effective quantities of a periodic medium with local stiffness $\mathbb{C}(\boldsymbol{x})$ in the context of a numerical homogenization process, a cubic RVE $\omega \in \mathbb{R}^3$ with periodic boundary conditions on $\partial\omega$ is considered. The local strain field is split into a prescribed constant macroscopic strain $\boldsymbol{E}$ and a fluctuation term $\boldsymbol{\varepsilon}(\boldsymbol{u}^*(\boldsymbol{x}))$.

$$\mathrm{div}\boldsymbol{\sigma}(\boldsymbol{x}) = \boldsymbol{0} \qquad\qquad\qquad \boldsymbol{x} \text{ on } \omega \tag{10a}$$

$$\boldsymbol{\sigma}(\boldsymbol{x}) = \left(1 - \bar{d}(\boldsymbol{x})\right) \mathbb{C}(\boldsymbol{x}) : \boldsymbol{\varepsilon}(\boldsymbol{x}) \qquad\qquad \boldsymbol{x} \text{ on } \omega \tag{10b}$$

$$\boldsymbol{\varepsilon}(\boldsymbol{x}) = \boldsymbol{E} + \frac{1}{2} \left(\bigtriangledown\boldsymbol{u}^*(\boldsymbol{x}) + (\bigtriangledown\boldsymbol{u}^*(\boldsymbol{x}))^T \right) \qquad \boldsymbol{x} \text{ on } \omega \tag{10c}$$

$$\boldsymbol{u}^*(\boldsymbol{x}) \quad \text{periodic} \qquad\qquad\qquad \boldsymbol{x} \text{ on } \partial\omega_D \tag{10d}$$

$$\boldsymbol{\sigma}(\boldsymbol{x}) \cdot \boldsymbol{n}(\boldsymbol{x}) \quad \text{anti-periodic} \qquad\qquad \boldsymbol{x} \text{ on } \partial\omega_N \tag{10e}$$

According to Zeller & Dederichs [20] the differential equation (10a) can be reformulated in an integral equation, the so called Lippmann-Schwinger equation, which is attributed to Lippmann & Schwinger [11] in the field of quantum mechanics. By introducing a homogeneous reference material with the stiffness $\mathbb{C}^0$, the polarization stress $\boldsymbol{\tau}$ with respect to this reference material the resulting constitutive equation read as follows:

$$\boldsymbol{\tau}(\boldsymbol{x}) = \left(1 - \bar{d}(\boldsymbol{x})\right) \mathbb{C}(\boldsymbol{x}) : \boldsymbol{\varepsilon}(\boldsymbol{x}) - \mathbb{C}^0 : \boldsymbol{\varepsilon}(\boldsymbol{x}) \tag{11}$$
$$\boldsymbol{\sigma}(\boldsymbol{x}) = \mathbb{C}^0 : \boldsymbol{\varepsilon}(\boldsymbol{x}) + \boldsymbol{\tau}(\boldsymbol{x}) . \tag{12}$$

The solution of the local problem in equation (10) can now be obtained using a nonlocal Green operator $\boldsymbol{\Gamma}^0$ which is applied on the stress polarization $\boldsymbol{\tau}$:

$$\boldsymbol{\varepsilon}(\boldsymbol{x}) = \boldsymbol{E} - \left(\boldsymbol{\Gamma}^0 * \boldsymbol{\tau}\right)(\boldsymbol{x}) . \tag{13}$$

The operator $\boldsymbol{\Gamma}^0$ is only associated with the stiffness of the homogenous linear elastic reference material $\mathbb{C}^0$ and the given boundary conditions, but does not depend on the fluctuating quantities [9]. The convolution (denoted by '$*$') in equation (13) is defined by:

$$\left(\boldsymbol{\Gamma}^0 * \boldsymbol{\tau}\right)(\boldsymbol{x}) = \int_{\omega} \boldsymbol{\Gamma}^0(\boldsymbol{x} - \boldsymbol{y}) : \boldsymbol{\tau}(\boldsymbol{y}) \, \mathrm{d}\boldsymbol{y} . \tag{14}$$

In the Fourier space it transforms into a direct product and the corresponding relation reads:

$$\hat{\boldsymbol{\varepsilon}}(\boldsymbol{\xi}) = -\hat{\boldsymbol{\Gamma}}^0(\boldsymbol{\xi}) : \hat{\boldsymbol{\tau}}(\boldsymbol{\xi}), \quad \forall \boldsymbol{\xi} \neq \boldsymbol{0}, \ \hat{\boldsymbol{\varepsilon}}(\boldsymbol{0}) = \boldsymbol{E} , \tag{15}$$

where $\hat{f}(\cdot)$ denotes a function in the Fourier space and $\boldsymbol{\xi}$ the Fourier space variable corresponding to the coordinates $\boldsymbol{x}$.
Substituting the expression of $\boldsymbol{\tau}$ (11) in (13) we arrive at a nonlinear Lippmann-Schwinger equation:

$$\boldsymbol{\varepsilon}(\boldsymbol{x}) = \boldsymbol{E} - \left(\boldsymbol{\Gamma}^0 * \left(\left((1 - \bar{d})\mathbb{C} - \mathbb{C}^0\right) : \boldsymbol{\varepsilon}\right)\right)(\boldsymbol{x}) . \tag{16}$$

There exist different numerical schemes to solve the Lippmann-Schwinger integral equation iteratively. In this work the so called basic scheme is used, which was introduced by Moulinec & Suquet [15]. The benefit of the scheme is based on the fact that the constitutive equation is solved in the real space and the convolution integral in the Fourier space. The transformation of the calculated fields is performed by a discrete fast Fourier transformation (FFT). Each iteration consists of four steps:

1. Solve the constitutive equation in the real space:
$$\boldsymbol{\tau}^i = \left((1 - \bar{d}^i)\mathbb{C} - \mathbb{C}^0\right) : \boldsymbol{\varepsilon}^i$$

2. Fourier transformation of the stress polarization field:
$$\hat{\boldsymbol{\tau}}^i = \mathrm{FFT}(\boldsymbol{\tau}^i)$$

3. Convolution with the Green operator in the Fourier space:
$$\hat{\boldsymbol{\varepsilon}}^{i+1} = -\hat{\boldsymbol{\Gamma}}^0 : \hat{\boldsymbol{\tau}}^i, \quad \hat{\boldsymbol{\varepsilon}}^{i+1}(0) = \boldsymbol{E}$$

4. Inverse Fourier transformation of the updated strain field:
$$\boldsymbol{\varepsilon}^{i+1} = \mathrm{FFT}^{-1}(\hat{\boldsymbol{\varepsilon}}^{i+1}) \quad .$$

According to [15] convergence is reached when the global stress field is in equilibrium:

$$\frac{\|\mathrm{div}\ \boldsymbol{\sigma}^{i+1}\|^2}{\|\boldsymbol{\sigma}^{i+1}\|^2} \leq\ \mathrm{tol}_1 \ , \tag{17}$$

which can easily be computed in the Fourier space:

$$\frac{\left\|\boldsymbol{\xi} \cdot \hat{\boldsymbol{\sigma}}^{i+1}(\boldsymbol{\xi})\right\|^2}{\left\|\hat{\boldsymbol{\sigma}}^{i+1}(\boldsymbol{0})\right\|^2} \leq \mathrm{tol}_1 \ . \tag{18}$$

Thereby $\hat{\boldsymbol{\sigma}}(\boldsymbol{0})$ equals the average or macroscopic stress and $\|\cdot\|^2$ denotes the L^2 norm of the appropriate field variable.

In this work a second convergence criterion is applied, which controls the difference of the strain field between two iterations in the real space (see e.g. [1]):

$$\frac{\|\boldsymbol{\varepsilon}^{i+1} - \boldsymbol{\varepsilon}^i\|^2}{\|\boldsymbol{E}\|^2} \leq\ \mathrm{tol}_2 \ . \tag{19}$$

Typical values for the convergence tolerances are $\mathrm{tol}_1 = 10^{-4}$ and $\mathrm{tol}_2 = 10^{-10}$.

The elastic parameters of the reference material $\mathbb{C}^0$, which have important influence on the convergence rate of the scheme, are chosen according to [15]:

$$k^0 = \frac{1}{2}\left(\min_{\boldsymbol{x}} k(\boldsymbol{x}) + \max_{\boldsymbol{x}} k(\boldsymbol{x})\right), \quad \mu^0 = \frac{1}{2}\left(\min_{\boldsymbol{x}} \mu(\boldsymbol{x}) + \max_{\boldsymbol{x}} \mu(\boldsymbol{x})\right) \ , \tag{20}$$

where μ and k denote shear and bulk modulus of an isotropic material.

It should be mentioned that in the last decade certain numerical schemes were developed to improve the convergence behavior of the FFT method for materials with high stiffness contrasts. A review of different schemes and an analysis of the convergence behavior for the computation of precise bounds of effective properties in comparison with analytical estimates can be found in [6].

3 MULTISCALE APPROACH

For the investigation of the macroscopic damage behavior the mesoscopic model is extended to a multiscale framework. Therefore the two scales are related to each other by a procedure similar to the FE^2 approach. Thus the constitutive equation on the macro scale is replaced by a BVP on the meso scale (see figure 1).
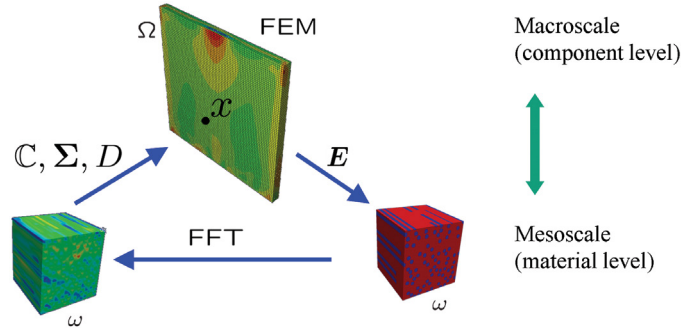
Figure 1: Scale coupling and multiscale approach schematically.

Each macroscopic point is linked to a RVE which represents the particular meso-structure at this point. The variables which are transferred between both scales are defined by volume averages over the meso domain:

$$\langle \cdot \rangle = \frac{1}{\omega} \int_\omega (\cdot)\, d\omega \ , \tag{21}$$

$$\boldsymbol{E} = \langle \boldsymbol{\varepsilon} \rangle, \quad \boldsymbol{\Sigma} = \langle \boldsymbol{\sigma} \rangle, \quad D = \langle d \rangle \ . \tag{22}$$

On the macroscale mixed BCs could be used and hence the macroscopic BVP reads as follows:

$$\text{div}\boldsymbol{\Sigma}(\boldsymbol{x}) = \boldsymbol{0} \qquad\qquad \boldsymbol{x} \text{ on } \Omega \tag{23a}$$

$$\boldsymbol{E}(\boldsymbol{x}) = \frac{1}{2}\left(\nabla \boldsymbol{U}(\boldsymbol{x}) + \nabla^T \boldsymbol{U}(\boldsymbol{x})\right) \qquad\qquad \boldsymbol{x} \text{ on } \Omega \tag{23b}$$

$$\boldsymbol{U}(\boldsymbol{x}) = \boldsymbol{U}_0(\boldsymbol{x}) \qquad\qquad \boldsymbol{x} \text{ on } \partial\Omega_D \tag{23c}$$

$$\boldsymbol{\Sigma}(\boldsymbol{x}) \cdot \boldsymbol{N}(\boldsymbol{x}) = \boldsymbol{T}_0(\boldsymbol{x}) \qquad\qquad \boldsymbol{x} \text{ on } \partial\Omega_N \ . \tag{23d}$$

The macroscopic BVP is solved using a standard Newton-Raphson scheme. Hence, in each macroscopic Newton iteration the averaged mesoscopic stresses $\langle \boldsymbol{\sigma} \rangle$ (for setting up the macroscopic residual force vector) and additionally for an efficient macro computation, the macroscopic tangential stiffness $\mathbb{C}^M$ has to be calculated. The latter is calculated by applying six infinitesimal perturbation loadcases to the current equilibrated solution according to [19, 13].

4   NUMERICAL EXAMPLES

The mesoscopic BVP stated in section 2 was implemented in the FFT code FeelMath developed at the Fraunhofer ITWM. In some numerical examples the mesomechanical damage behavior and the scale coupling technique are illustrated.

4.1   Mesoscale Simulation of a Fiber Composite

The following example demonstrates the behavior of the mesoscopic damage model using a short fiber reinforced composite which is discretized by 384,000 voxel cells. The behavior of the glass fibers is assumed to be linear elastic while for the polymer matrix the nonlocal damage model described in section 2.1 is used. The structure is loaded with periodic deformation BCs.
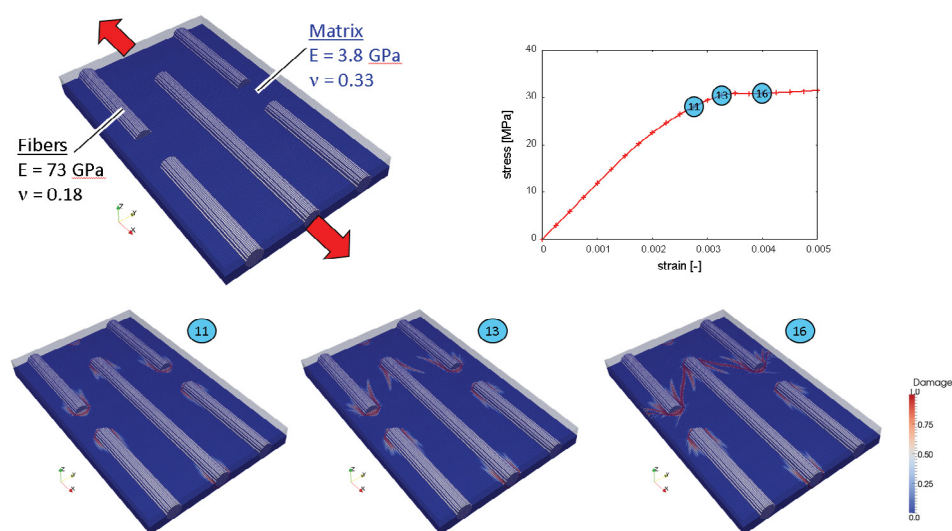
Figure 2: Damage evolution on the mesoscale demonstrated on the example of a short fiber reinforced composite.

As illustrated in figure 2 the damage starts to grow on the sharp fiber edges and increases along the fiber matrix interface. With increasing load, shear bands occur between the fibers which connect the separated damage zones around the fibers. This results finally in a continuously meso crack and consequently in a complete failure of the meso structure.

1208

4.2 Detection of the Onset of Macroscopic Localization

As already mentioned, at a certain point during the load history the macroscopic strain starts to localize and the problem becomes ill-posed. This point, which can be regarded as the onset of macroscopic failure, is detected by an acoustic analysis of the current homogenized tangent stiffness tensor [5, 17]. Therefore the acoustic tensor $\boldsymbol{A}(\boldsymbol{n})$ is calculated by applying the normal vectors $\boldsymbol{n}$ for all possible angles (φ and θ) on the macro tangent [3]:

$$
\begin{aligned}
A_{jk}(\boldsymbol{n}) &= C_{ijkl}^{M} n_i n_l \,, & (24) \\
\boldsymbol{n} &= \boldsymbol{n}(\varphi, \theta) \,, & (25) \\
\|\boldsymbol{n}\| &= 1 \,, & (26)
\end{aligned}
$$

where the definition of the acoustic tensor $\boldsymbol{A}$ is given in index notation. Localization occurs if the following criterion is fulfilled for a certain direction $\boldsymbol{n}$:

$$
\det\left(\boldsymbol{A}(\boldsymbol{n})\right) = 0 \,. \tag{27}
$$

We demonstrate this analysis on a cubic RVE containing a single linear elastic fiber inclusion. The structure is discretized by 75^3 (421,875) voxel cells and loaded during 10 time steps with a uniaxial macroscopic strain perpendicular to the fiber direction. In this example the nonlocal part of the damage model is suppressed to demonstrate the localization effect during the applied load history. In each time step we compute the homogenized macroscopic tangent and the acoustic tensor determinant for all directions.
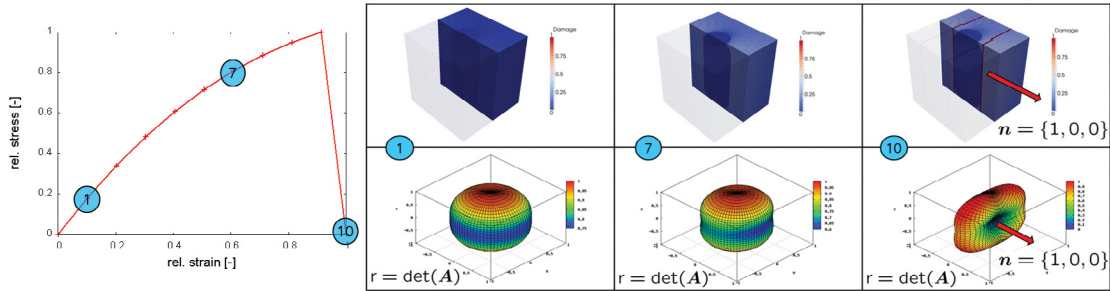

Figure 3: Detection of the onset of macroscopic failure with the acoustic tensor.

In figure 3 the normalized determinant of the acoustic tensor is plotted using spherical coordinates. Thereby the value of the determinant illustrated as the spherical radius decreases with growing damage in the direction perpendicular to the crack direction.

4.3   Multiscale Simulation of a Fiber Composite

In figure 4 an example for a fully coupled multiscale approach is demonstrated. A strip with a hole discretized by 516 tetrahedral finite elements is coupled to a short fiber reinforced RVE structures which are modeled with 64^3 (262144) voxel cells. The macroscopic linear elastic material behavior is replaced in some critical regions with a coupled multiscale approach. RVEs with 45° and 90° fiber orientation with respect to the macro loading direction are associated to particular macroscopic regions. The polymer matrix is modeled by the nonlocal damage model described in section 2.1 and the behavior of the fibers is assumed to be linearly elastic.
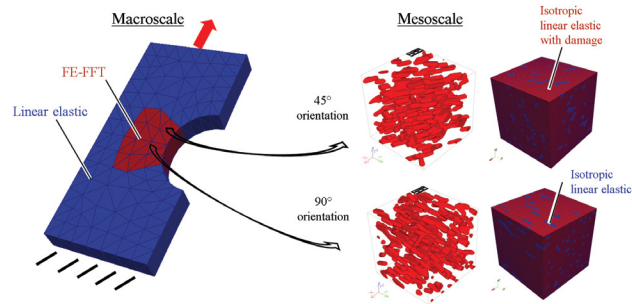
Figure 4: Fully coupled meso-macro computation of a strip with a hole and short fiber reinforced composite material structures.

Damage is captured on the finer scale which is illustrated in figure 5 for both fiber mesostructures. Growing damage on the fine scale with an increasing macroscopic load results in macroscopic reduction of stiffness. The maximal stresses move from the vicinity of the hole towards the center of the specimen. The meso- and macroscopic stress-strain response both show a nonlinear material behavior.
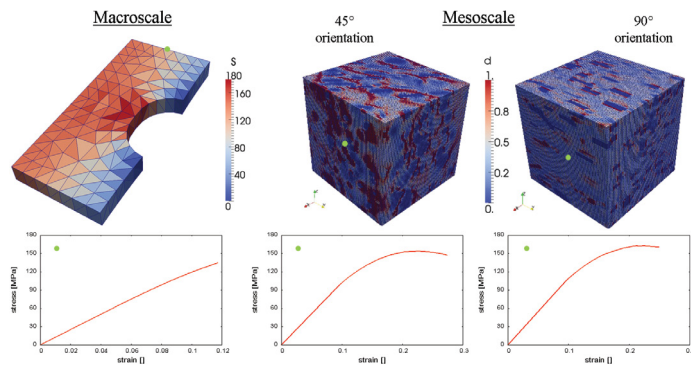
Figure 5: Stiffness reduction around the hole of the macroscopic specimen due to increasing damage on the mesoscale.

5 CONCLUSIONS

In this work we proposed an alternative multiscale approach similar to FE^2 to investigate progressive damage behavior of composite materials. Nonlinear material effects caused by mesoscopic physical effects were modeled on a finer length scale and used to predict the macroscopic damage behavior.

In the first numerical example a meso scale problem was set up to demonstrate the behavior of the mesoscopic model. In this context we illustrated the mechanisms of growing damage which can be observed in short fiber reinforced composites.

Further we showed a simple way to predict the onset of macroscopic failure. We carried out an acoustic analysis of the current effective tangent stiffness tensor which was obtained by homogenization of a RVE around different macroscopic load states.

Finally, in the third numerical example a coupled multiscale simulation was performed. The elastic material behavior of a strip with a hole was replaced in some critical regions with a multiscale approach to model progressive damage on the coarse scale. Growing damage which occurred at the fine scale between the material constituents resulted in macroscopic reduction of stiffness and redistribution of macroscopic stresses.

REFERENCES

[1] S. Brisard and L. Dormieux. FFT-based methods for the mechanics of composites: A general variational framework. *Computational Materials Science*, 49(3):663–671, 2010.

[2] R.H.J.P.R. DE and JHP DE VREE. Gradient enhanced damage for quasi-brittle materials. *International Journal for Numerical Methods in Engineering*, 39:3391–3403, 1996.

[3] R De Borst, LJ Sluys, H-B Muhlhaus, and Jerzy Pamin. Fundamental issues in finite element analyses of localization of deformation. *Engineering computations*, 10(2):99–121, 1993.

[4] F. Feyel and J.L. Chaboche. FE^2 multiscale approach for modelling the elastoviscoplastic behaviour of long fibre SiC/Ti composite materials. *Computer methods in applied mechanics and engineering*, 183(3):309–330, 2000.

[5] Rodney Hill. Acceleration waves in solids. *Journal of the Mechanics and Physics of Solids*, 10(1):1–16, 1962.

[6] M. Kabel and H. Andrä. Numerical bounds of effective elastic moduli. *Berichte des Fraunhofer ITWM*, 224(1):1–13, 2012.

[7] L. Kachanov. *Introduction to continuum damage mechanics*, volume 10. Springer, 1986.

[8] P. Kanouté, DP Boso, JL Chaboche, and BA Schrefler. Multiscale methods for composites: a review. *Archives of Computational Methods in Engineering*, 16(1):31–75, 2009.

[9] E. Kröner. Bounds for effective elastic moduli of disordered materials. *Journal of the Mechanics and Physics of Solids*, 25(2):137–155, 1977.

[10] Jean Lemaitre and Rodrigue Desmorat. *Engineering damage mechanics: ductile, creep, fatigue and brittle failures.* Springer, 2005.

[11] B.A. Lippmann and J. Schwinger. Variational principles for scattering processes. I. *Physical Review*, 79(3):469, 1950.

[12] J. Mazars and G. Pijaudier-Cabot. Continuum damage theory-application to concrete. *Journal of Engineering Mechanics*, 115(2):345–365, 1989.

[13] Christian Miehe. Numerical computation of algorithmic (consistent) tangent moduli in large-strain computational inelasticity. *Computer Methods in Applied Mechanics and Engineering*, 134(3):223–240, 1996.

[14] H. Moulinec and P. Suquet. A fast numerical method for computing the linear and nonlinear mechanical properties of composites. *Comptes rendus de l'Académie des sciences. Série II, Mécanique, physique, chimie, astronomie*, 318(11):1417–1423, 1994.

[15] H. Moulinec and P. Suquet. A numerical method for computing the overall response of nonlinear composites with complex microstructure. *Computer Methods in Applied Mechanics and Engineering*, 157(1):69–94, 1998.

[16] G. Pijaudier-Cabot and Z.P. Bazant. Nonlocal damage theory. *Journal of Engineering Mechanics*, 113(10):1512–1533, 1987.

[17] JR Rice and JW Rudnicki. A note on some features of the theory of localization of deformation. *International Journal of solids and structures*, 16(7):597–605, 1980.

[18] JC Simo and JW Ju. Strain-and stress-based continuum damage models-I. Formulation. *International journal of solids and structures*, 23(7):821–840, 1987.

[19] Ilker Temizer and Peter Wriggers. On the computation of the macroscopic tangent for multiscale volumetric homogenization problems. *Computer Methods in Applied Mechanics and Engineering*, 198(3):495–510, 2008.

[20] R. Zeller and PH Dederichs. Elastic constants of polycrystals. *Physica status solidi (b)*, 55(2):831–842, 1973.